Uluslararası İleri Doğa Bilimleri ve Mühendislik Araştırmaları Dergisi
Sayı 8, S. 207-214, 6, 2024

Araştırma Makalesi

IJANSER

https://as-proceeding.com/index.php/ijanser
ISSN: 2980-0811

International Journal of Advanced Natural Sciences and Engineering Researches
Volume 8, pp. 207-214, 6, 2024

Research Article

Predicting Load-Carrying Capacity of FRP-Confined CFST Columns through Analytical Techniques

Mehar Ali[*], Muhammad Umair Raza [2], Mohammad Hasnat Akbar khan [3], Muhammad Hassan [4],

Sultan Arshid [5], Emaan Yousaf [6,] Hassan Akhter [7] and Ali Raza [8]

[1,2,3,4,5,6,7,8]*Department of Civil Engineering, University of Engineering and Technology Taxila, 47050,* Pakistan

Email of the corresponding author: (meharaliali25@gmail.com)

(Received: 23 July 2024, Accepted: 24 July 2024)

(4th International Conference on Scientific and Academic Research ICSAR 2024, July 19 - 20, 2024)

ATIF/REFERENCE: Ali, M., Raza, M. U., Akbar khan, M. H., Hassan, M., Arshid, S., Yousaf, E., Akhter, H. & Raza, A. (2024). Predicting Load-Carrying Capacity of FRP-Confined CFST Columns through Analytical Techniques. *International Journal of Advanced Natural Sciences and Engineering Researches*, 8(6), 207-214.

Abstract – While earlier research has used sparse and imprecise data to study the load-carrying capacity (LC) prediction of fiber-reinforced polymer (FRP)-confined concrete-filled steel tube (CFST) compression members (SFC), no study has examined the predictive accuracy of different modeling approaches using an extensive and refined database. The purpose of this work is to present an analytical model for LC prediction of SFC compression members. The confinement mechanics of steel tubes and FRP wraps are included in the model, which was created using a database of 712 samples. The analytical model yields precise predictions by considering the lateral confinement mechanism of SFC columns. For the LC of SFC columns, statistical metrics of MAE = 427.23, MAPE = 283.65, R2 = 0.815, RMSE = 275.43, and a20-index = 0.73 are obtained by evaluation using the experimental database.

Keywords – CRFP, CFST, Analytical Model, Load-Carrying Capacity.

I. INTRODUCTION

When restricted with steel tube (ST) and fiber-reinforced polymers (FRP), concrete compression members demonstrate remarkable mechanical performance and adaptability. In civil engineering projects involving long-span bridges and multistory buildings, these members come highly recommended. Because of its various qualities, including superior mechanical qualities, resistance to high temperatures, great durability, low maintenance costs, and good resistance to corrosive environments, stainless steel is typically used over carbon steel in the manufacturing of concrete. When externally confined, stainless steel provides concrete compression members with higher axial compressive strength. But when these members potentially buckle, the effectiveness of stainless steel is undermined, which lowers the material's ductility and load-bearing capability. It is advised to use FRP sheets to reduce lateral buckling by offering more lateral confinement, which will increase the axial stiffness of the ST and solve these problems. Concrete compression members' ductility and axial compression strength are both significantly increased with improved confinement, which enhances the seismic performance of the components.

The axial compressive performance of conventional ST and/or stainless-ST compression members exposed to confinement with and without FRP wraps has been evaluated through a number of experimental

investigations. The axial strength and strain of concrete compression members with improved confinement from the combination of FRP and ST, which increases the core resistance against lateral buckling, have been significantly improved, according to these investigations. Compression members have more ductility and load-bearing strength as a result of this enhancement. The interdependency between confining stresses and strains is demonstrated by the changes in the confined concrete microstructure brought about by confinement, which affect both the confined concrete stress and splitting cracking in the core concrete.

However, due to noisy results and a small dataset, analytical modeling estimates have not been precise enough to describe the complexity of several factors of FRP-confined concrete compression components. Consequently, a substantial experimental record encompassing a range of factors for FRP-confined samples is needed to obtain reliable estimates from analytical models.The load-carrying capacity (LC) of FRP-confined CFST compression members (SFC) was estimated using restricted experimental data in earlier analytical models, which did not sufficiently account for the factors unique to FRP confinement, such as the interaction between the FRP wraps, ST, and concrete. Therefore, more study will be needed to create a more thorough model that can estimate the load-bearing capacity of SFC compression members. Regression analysis-based analytical modeling with an experimental database was utilized by the authors of this study to assess the SFC compression members' performance. An analytical model that takes into account all of the FRP and ST confining mechanisms as well as a database of 712 FRP-confined samples was suggested to predict the LC of SFC compression components.

II. ANALYTICAL MODELLING

a. DATABASE

Table 1 provides the database gathered from various experimental tests conducted on the FRP-confined concrete specimens. Different parameters of FRP-confined samples were considered such as diameter of sample (D), height of sample (H), confined concrete compressive strength (f'_{cc}), elastic modulus of FRPs (E_f), unconfined concrete compressive strength (f'_{co}), unconfined concrete strain (ε_{co}), thickness of FRP sheets (nt), and confined concrete strain (ε_{cc}). Steel tube confinement was considered in the form of external pressure mechanics of compressive samples. The validation of proposed model was carried out based on the database of 325 CFST columns (presented in Table 2). Where f_f is the tensile strength of FRP sheets, ε_s is the strain of steel tube, ε_f is the strain of FRP sheets, A is the cross-sectional area of column, t_s is the thickness of steel tube, f_s is the yield strength of steel tube, and P is the axial load-carrying capacity of CFST column.

Table 1. Database for FRP-confined samples

Parameter	D (mm)	H (mm)	nt (mm)	E_f (GPa)	f'_{co} (MPa)	f'_{cc} (MPa)	ε_{co} (%)	ε_{cc} (%)
MIN	51	102	0.09	10	12.41	18.5	0.1676	0.083
MAX	406	812	5.9	663	188.2	302.2	1.53	4.62
Mean	153.37	306.94	0.88	172.03	41.97	75.58	0.27	1.52
St.Dev	42.99	85.99	1.04	119.61	22.47	35.17	0.14	0.86
COV	0.29	0.29	1.19	0.7	0.54	0.47	0.52	0.57

Table 2. Database for CFST columns

Parameter	A (mm^2)	H (mm)	f'_{co} (MPa)	t_s (mm)	f_s (MPa)	ε_s (%)	f_f (MPa)	E_f (GPa)	ε_f (%)	nt (mm)	P (kN)
MIN	7200	300	28	0.67	1.23	0.01	250	13.9	0.01	0	478
MAX	125600	2000	140	8.8	729.7	5	4598	272.9	4.56	30	9358
Mean	21700.69	488.47	48.37	4.29	329.43	0.48	3076.56	184.08	0.75	1.28	2154.03
St.Dev	21310.16	293.26	27.13	1.96	150.36	1.12	1156.07	86.14	0.9	2.81	1742.76
COV	0.98	0.6	0.56	0.46	0.46	2.33	0.38	0.47	1.2	2.2	0.81

III. ASSESMENT OF PREVIOUS MODELS

An extensive assessment of the literature indicates a deficiency of studies on the use of analytical models to assess the load-carrying capacity (LC) of SFC compression components. Traditionally, finite element analysis (FEA) results or tiny experimental databases have been the basis for existing models [29], frequently with incomplete consideration of the confining mechanism. But this work presents a new analytical model that is based on a large experimental database with 325 samples. The model considers the potential confining effect of ST, CFRP wraps, and their axial effects.

The database was created with research that had already been published and was updated to eliminate noisy datasets that could cause errors in the best-fit curves that were greater than 20%. Using the created database, a number of analytical models [38–43] that have previously been applied to restricted concrete samples were examined for correctness and generic form. The stress-path of the confining material has a major impact on the strength of confined concrete, which is concrete that is contained within a ST. There is a lag between the confining strain and the axial strain and stress in stiffer concrete as compared to normal strength concrete because stiffer concrete shows slower fracture propagation for different concrete strengths.

By taking into account the compression strength of the core concrete with CFRP wraps, the LC of SFC compression members may be approximated using the external confining mechanism of ST. The established database is consulted in order to determine the axial compression strength of core concrete with CFRP layers (P_{cc}). Analytical formulas are employed to find the LC with the external restricting action of ST (P_{st}). The created database was used to assess the chosen analytical models for the LC of CFRP-confined concrete [38–43]. In the end, this method aids in improving the model's form using a number of statistical variables, which are derived from Equations (1-5) and include mean absolute error (MAE), determination coefficient (R^2), root mean squared error (RMSE), and a20-index. Here, n indicates the total number of samples, x_i represents the experimental results, and y_i denotes the estimated results.

$$MAE = \frac{1}{n}\sum_{i=1}^{n}|x_i - y_i| \tag{1}$$

$$R^2 = \left(\frac{n(\sum_{i=1}^{n} x_i y_i) - (\sum_{i=1}^{n} x_i)(\sum_{i=1}^{n} y_i)}{\sqrt{[n\sum_{i=1}^{n} {x_i}^2 - (\sum_{i=1}^{n} x_i)^2][n\sum_{i=1}^{n} {y_i}^2 - (\sum_{i=1}^{n} y_i)^2]}}\right)^2 \tag{2}$$

$$MAPE = \frac{1}{n}\sum_{i=1}^{n}\left|\frac{x_i - y_i}{x_i}\right| \tag{3}$$

$$RMSE = \sqrt{\frac{1}{n}\sum_{i=1}^{n}(x_i - y_i)^2} \tag{4}$$

$$a_{20} - index = \frac{N_{20}}{n} \tag{5}$$

The number of samples where the "experimental value" to "predicted value" ratio is between 0.80 and 1.20 is indicated by the notation N_{20}. It is significant to remember that the a20-index would be 1 in a perfect prediction model. The suggested a20-index indicates the proportion of samples in which the expected values differ by ±20% from the experimental values, offering a useful engineering interpretation.

The strength model suggested by Lam and Teng [47] produced the best results over the experimental dataset, with an R2 of 0.903 and an RMSE of 0.244, after the other models under examination were compared. As a result, this strength model has been used for regression analysis as well as curve fitting, producing the best results for the LC of SFC compression members. The results of the various models' assessments are shown in Figure 1.

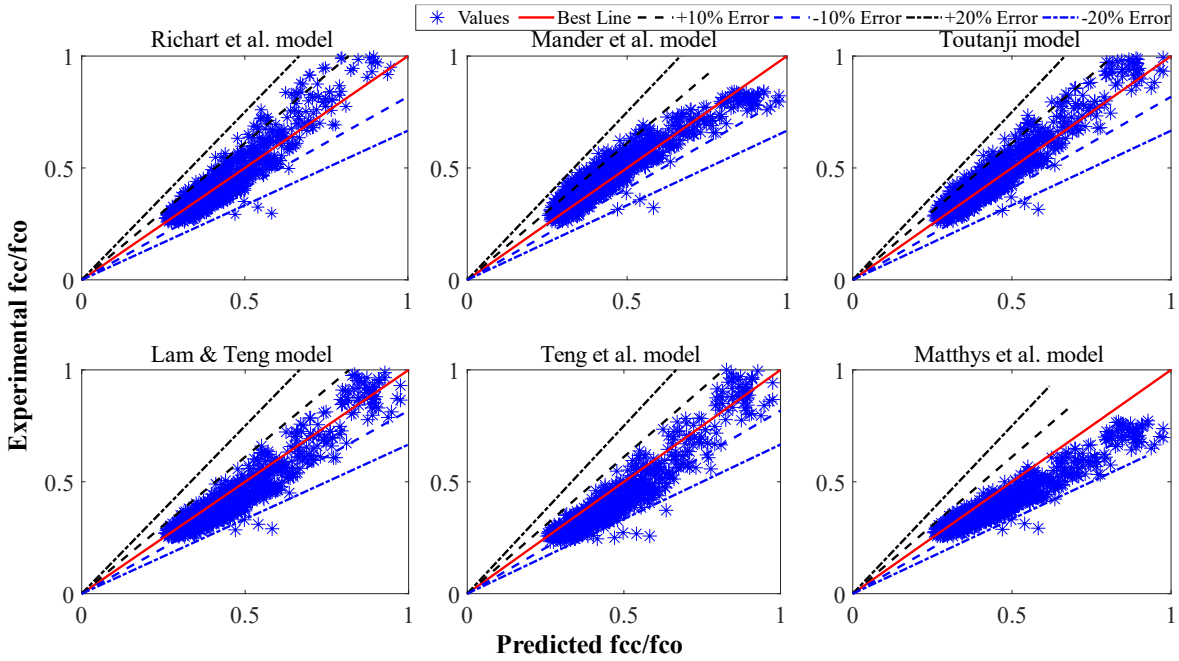

Figure 1. The performance evaluation of various models

IV. PROPOSED MODEL

The LC of SFC compression members (P_n) can be computed by adding the axial compression strength sourced from the external confinement from the ST (P_{st}) and axial compressive strength of core concrete subjected to confining action given by CFRP sheets (P_{cc}).

$$P_n = P_{cc} + P_{st} \tag{6}$$

The axial compression strength of concrete can be defined as $P_{cc} = A_{cc} f'_{cc}$, where A_{cc} designates the core concrete area confined with CFRP layers while f'_{cc} presents the compression strength of concrete core. Eq. (7) reports the form of the recently established model for the axial compression strength of core concrete having CFRP wraps.

$$f'_{cc} = f'_{co} + k f'^{1-n}_{co} f_l^{\,n} \tag{7}$$

Here f_l represents the ultimate confinement stress as proved to the core concrete by CFRP wraps. The calibrated k and n values of the constants were discovered by using MATLAB to minimize the statistical concerns and to find the best fit curve (R^2) over the dataset. According to the results of the regression analysis, k had a value of 3.1 and n was 0.83. The final expression of the expression for the axial compression strength of core concrete under CFRP confinement is shown in Eq. (8).

$$f'_{cc} = f'_{co} + 3.1 f'^{0.22}_{co} f_l^{0.83} \quad (8)$$

Figure 2 shows the model's performance over the created experimental dataset, with RMSE = 0.18 and R^2 = 0.94. These parameters show that this model produced better outcomes than the previously employed models.

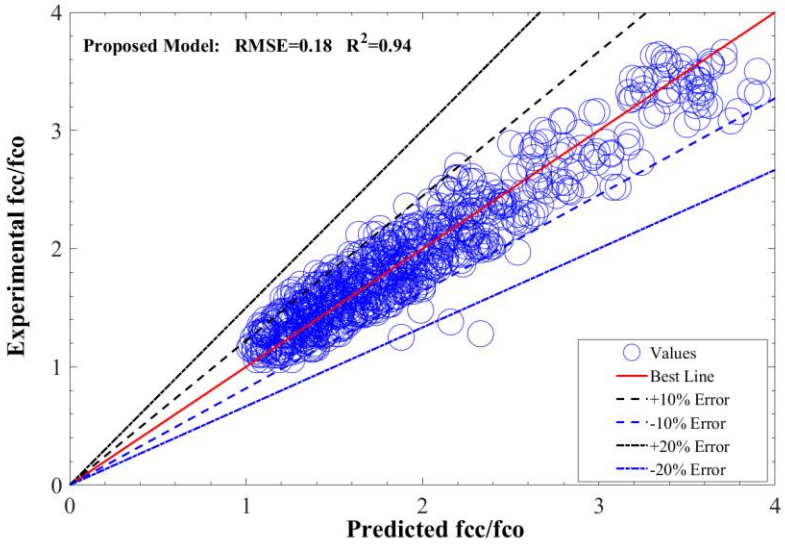

Figure 2. Evaluation of proposed strength model for FRP-confined concrete strength (f'_{cc}).

Hence, to better understand the behavior of axial compression strength of core concrete under CFRP wraps (P_{cc}) Eq. (9) can be referred:

$$P_{cc} = A_{cc}\left[f'_{co} + 3.1 f'^{0.22}_{co} f_l^{0.83}\right] \quad (9)$$

Likewise, to evaluate the axial compression strength with the external confining mechanism from the ST (P_{st}) Eq. (10) can be used which acknowledges both the strain hardening as well as the resistances of ST subjected to the axial shortening by adopting the continuous strength approach [29, 48, 49].

$$P_{st} = A_{st}\sigma_{LB} \quad (10)$$

In this equation, A_{st} expresses the ST cross-sectional area whereas σ_{LB} presents stress explaining the localized buckling action of the tube. Characteristics of the strain hardening characteristics of ST primarily support the influence of ST in the LC and ductility of SFC compression members [50]. The parameter σ_{LB} can be obtained with following expressions [49]:

$$\sigma_{LB} = E\varepsilon_{LB}\frac{\varepsilon_{LB}}{\varepsilon_{0.2}} < 1.0 \quad (11)$$

$$\sigma_{LB} = \varepsilon_{0.2} + E_{sh}\varepsilon_{0.2}\left(\frac{\varepsilon_{LB}}{\varepsilon_{0.2}} - 1\right)\frac{\varepsilon_{LB}}{\varepsilon_{0.2}} \geq 1.0 \quad (12)$$

In this equation, ε_{LB} defines the local buckling action, E depicts the elasticity and $\varepsilon_{0.2}$ represents the 2% strain of the tube. Similarly, E_{sh} explains the elasticity of ST observed while the biaxial strain hardening

process is executed. Buchanan and Gardner [49] followed a model to develop the association of deformation capacity (λ_c) with the cross-sectional slenderness of tube and is expressed by Eq. (13).

$$\frac{\varepsilon_{LB}}{\varepsilon_{0.2}} = \frac{4.44 \times 10^{-3}}{\lambda_c^{4.5}} \leq minimum(15, \frac{0.1\varepsilon_u}{\varepsilon_{0.2}}) \quad (13)$$

Here, ε_u defines the highest strain of the ST. To conclude, the established model for the LC of SFC compression members can be described by Eq. (14) which explicitly considers the axial impact of ST, CFRP wraps, and their confining actions.

$$P_n = A_{cc}f'_{cc} + A_{st}\sigma_{LB} = A_{cc}\left[f'_{co} + 3.1f'^{0.22}_{co}f_l^{0.83}\right] + A_{st}\sigma_{LB} \quad (14)$$

The proposed analytical model for predicting the LC of SFC columns showed the statistics with a20-index of 0.73, an RMSE of 275.43, an MAE of 427.23, R^2 of 0.815, and a MAPE of 283.65 based on the experimental database of 325 SFC compression members. Figure 3 shows the predictions of proposed analytical model (Eq. 14) for LC of SFC compression members.

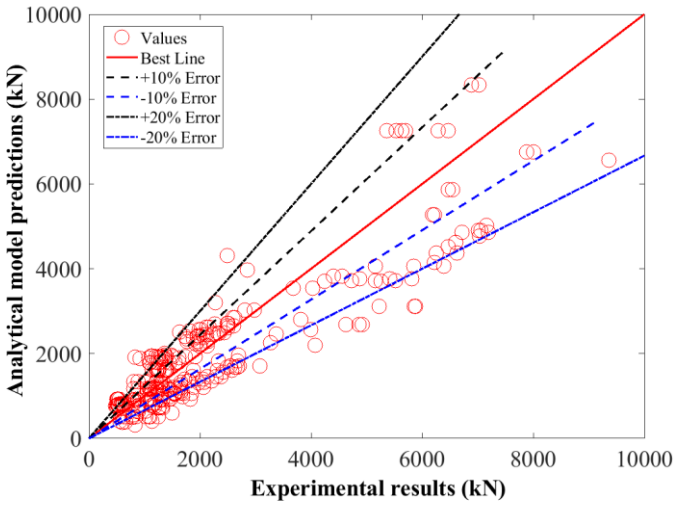

Figure 3. Predictions for the proposed model for LC of SFC columns

V. CONCLUSION

The purpose of this study was to forecast the load-carrying capacity (LC) of concrete-filled (SFC) compression members with fiber-reinforced polymer (FRP) confined steel tube (ST). With the use of a sizable experimental dataset of 712 samples, it carried out a thorough analytical modeling backed by regression analysis and curve fitting. Based on confinement mechanics and several previously used models for CFRP-confined strength over the dataset, the analytical model used for the LC of the SFC columns was created. With an a20-index of 0.73, an RMSE of 275.43, an MAE of 427.23, and a MAPE of 283.65, the model demonstrated good agreement with the experimental results. The constraining action of both CFRP wraps and ST was explicitly considered in this model, which shows improved accuracy over earlier models.

REFERENCE

1. Han, L.-H., W. Li, and R. Bjorhovde, Developments and advanced applications of concrete-filled steel tubular (CFST) structures: Members. Journal of constructional steel research, 2014. **100**: p. 211-228.
2. Raza, A., et al., Rapid repair of geopolymer concrete members reinforced with polymer composites: Parametric study and analytical modeling. Engineering Structures, 2024. **299**: p. 117143.
3. Zhang, B., et al., Seismic behaviour of FRP-concrete-steel double-tube columns with shear studs: Experimental study and numerical modelling. Engineering Structures, 2024. **302**: p. 117339.

4. Zhang, B., et al., Elliptical concrete-filled FRP tubes with an embedded H-shaped steel under axial compression and cyclic lateral loading: Experimental study and modelling. Composite Structures, 2024. **330**: p. 117839.
5. Raza, A., et al. Axial performance of GFRP composite bars and spirals in circular hollow concrete columns. in Structures. 2021. Elsevier.
6. Raza, A., et al., Structural performance of FRP-RC compression members wrapped with FRP composites. Structures, 2020. **27**: p. 1693-1709.
7. Raza, A., et al. Performance evaluation of hybrid fiber reinforced low strength concrete cylinders confined with CFRP wraps. in Structures. 2021. Elsevier.
8. Raza, A., et al. Prediction of axial load-carrying capacity of GFRP-reinforced concrete columns through artificial neural networks. in Structures. 2020. Elsevier.
9. Raza, A., et al., Finite element modelling and theoretical predictions of FRP-reinforced concrete columns confined with various FRP-tubes. Structures, 2020. **26**: p. 626-638.
10. Fam, A., F.S. Qie, and S. Rizkalla, Concrete-filled steel tubes subjected to axial compression and lateral cyclic loads. Journal of Structural Engineering, 2004. **130**(4): p. 631-640.
11. O'Shea, M.D. and R.Q. Bridge, Design of circular thin-walled concrete filled steel tubes. Journal of Structural Engineering, 2000. **126**(11): p. 1295-1303.
12. Xiao, Y., Applications of FRP composites in concrete columns. Advances in Structural Engineering, 2004. **7**(4): p. 335-343.
13. Chen, Z., S. Dong, and Y. Du, Experimental study and numerical analysis on seismic performance of FRP confined high-strength rectangular concrete-filled steel tube columns. Thin-Walled Structures, 2021. **162**: p. 107560.
14. Cao, S., C. Wu, and W. Wang, Behavior of FRP confined UHPFRC-filled steel tube columns under axial compressive loading. Journal of Building Engineering, 2020. **32**: p. 101511.
15. NadimiShahraki, K. and M. Reisi. Stress-strain based method for analysis and design of FRP wrapped reinforced concrete columns. in Structures. 2020. Elsevier.
16. Feng, C., F. Yu, and Y. Fang. Mechanical behavior of PVC tube confined concrete and PVC-FRP confined concrete: A review. in Structures. 2021. Elsevier.
17. Zakir, M., F.A. Sofi, and J.A. Naqash. Experimentally verified behavior and confinement model for concrete in circular stiffened FRP-concrete-steel double-skin tubular columns. in Structures. 2021. Elsevier.
18. Teng, J., et al., Three-dimensional finite element analysis of reinforced concrete columns with FRP and/or steel confinement. Engineering Structures, 2015. **97**: p. 15-28.
19. Zeng, L., et al., Experimental study of seismic performance of full-scale basalt FRP-recycled aggregate concrete-steel tubular columns. Thin-Walled Structures, 2020. **151**: p. 106185.
20. Cai, J., et al., Behavior of geopolymeric recycled aggregate concrete-filled FRP tube (GRACFFT) columns under lateral cyclic loading. Engineering Structures, 2020. **222**: p. 111047.
21. Giakoumelis, G. and D. Lam, Axial capacity of circular concrete-filled tube columns. Journal of Constructional Steel Research, 2004. **60**(7): p. 1049-1068.
22. Lam, D. and L. Gardner, Structural design of stainless steel concrete filled columns. Journal of Constructional Steel Research, 2008. **64**(11): p. 1275-1282.
23. Liew, J.R. and D. Xiong, Effect of preload on the axial capacity of concrete-filled composite columns. Journal of Constructional Steel Research, 2009. **65**(3): p. 709-722.
24. Han, L.-H., W. Li, and R. Bjorhovde, Developments and advanced applications of concrete-filled steel tubular (CFST) structures: Members. Journal of Constructional Steel Research, 2014. **100**: p. 211-228.
25. Tam, V.W., Z.-B. Wang, and Z. Tao, Behaviour of recycled aggregate concrete filled stainless steel stub columns. Materials Structures, 2014. **47**(1-2): p. 293-310.
26. Perea, T., et al., Full-scale tests of slender concrete-filled tubes: Interaction behavior. Journal of Structural Engineering, 2014. **140**(9): p. 04014054.
27. Ding, F.-x., et al., Mechanical behavior of circular and square concrete filled steel tube stub columns under local compression. Thin-Walled Structures, 2015. **94**: p. 155-166.
28. Liu, J.-P., et al., Axial behaviour of circular steel tubed concrete stub columns confined by CFRP materials. Construction Building Materials, 2018. **168**: p. 221-231.
29. Sharif, A.M., G.M. Al-Mekhlafi, and M.A. Al-Osta, Structural performance of CFRP-strengthened concrete-filled stainless steel tubular short columns. Engineering Structures, 2019. **183**: p. 94-109.
30. Xu, T., J. Liu, and Y. Guo, Design method of short circular FRP-steel composite tubed RC columns under eccentric compression. Composite Structures, 2020: p. 113359.
31. Wang, Y.-H., et al., Coupled ultimate capacity of CFRP confined concrete-filled steel tube columns under compression-bending-torsion load. Structures, 2021. **31**: p. 558-575.
32. Yang, J., et al., Behavior of eccentrically loaded circular CFRP-steel composite tubed steel-reinforced high-strength concrete columns. Journal of Constructional Steel Research, 2020. **170**: p. 106101.
33. Hameed, M.H., A.H.A. Al-Ahmed, and Z.K. Abbas, Enhancing the strength of reinforced concrete columns using steel embedded tubes. Mechanics of Advanced Materials and Structures, 2020: p. 1-16.

34. Zhang, Y.-f. and Z.-q. Zhang, Study on equivalent confinement coefficient of composite CFST column based on unified theory. Mechanics of Advanced Materials and Structures, 2016. **23**(1): p. 22-27.
35. Dong, C., A. Kwan, and J. Ho, A constitutive model for predicting the lateral strain of confined concrete. Engineering Structures, 2015. **91**: p. 155-166.
36. Kwan, A., C. Dong, and J. Ho, Axial and lateral stress–strain model for FRP confined concrete. Engineering Structures, 2015. **99**: p. 285-295.
37. Lai, M., L. Hanzic, and J.C. Ho, Fillers to improve passing ability of concrete. Structural Concrete, 2019. **20**(1): p. 185-197.
38. Mander, J.B., M.J. Priestley, and R. Park, Theoretical stress-strain model for confined concrete. Journal of structural engineering, 1988. **114**(8): p. 1804-1826.
39. Lam, L. and J.G. Teng, Design-oriented stress–strain model for FRP-confined concrete. Construction and building materials, 2003. **17**(6-7): p. 471-489.
40. Toutanji, H., Stress-strain characteristics of concrete columns externally confined with advanced fiber composite sheets. Materials Journal, 1999. **96**(3): p. 397-404.
41. Teng, J., et al., Refinement of a design-oriented stress–strain model for FRP-confined concrete. Journal of composites for construction, 2009. **13**(4): p. 269-278.
42. Richart, F., A. Brandtzaeg, and R. Brown, The failure of plain and spirally reinforced concrete in compression. Bulletin 190. University of Illinois Engineering Experimental Station, Illinois, 1929.
43. Matthys, S., et al., Axial load behavior of large-scale columns confined with fiber-reinforced polymer composites. ACI Structural Journal, 2005. **102**(2): p. 258.
44. Lai, M., et al., A stress-path dependent stress-strain model for FRP-confined concrete. Engineering Structures, 2020. **203**: p. 109824.
45. Lai, M., et al., A path dependent stress-strain model for concrete-filled-steel-tube column. Engineering Structures, 2020. **211**: p. 110312.
46. Ho, J., et al., A path dependent constitutive model for CFFT column. Engineering Structures, 2020. **210**: p. 110367.
47. Lam, L. and J. Teng, Design-oriented stress–strain model for FRP-confined concrete. Construction Building Materials, 2003. **17**(6-7): p. 471-489.
48. Zhao O, A.S., Gardner L, Structural response and continuous strength method design of slender stainless steel cross-sections. Engineering Structures, 2017. **140**: p. 14-25.
49. Buchanan C, G.L., Liew A, The continuous strength method for the design of circular hollow sections. Journal of Constructional Steel Research, 2016. **118**: p. 207-16.
50. Tao, Z., et al., Nonlinear analysis of concrete-filled square stainless steel stub columns under axial compression. Journal of Constructional Steel Research, 2011. **67**(11): p. 1719-1732.